“Babeş-Bolyai” University Cluj-Napoca
Faculty of Biology and Geology
Department of Geology

Epithermal processes related to Neogene andesite intrusions in the Certej area (Apuseni Mountains, Romania)

Ph.D. thesis abstact

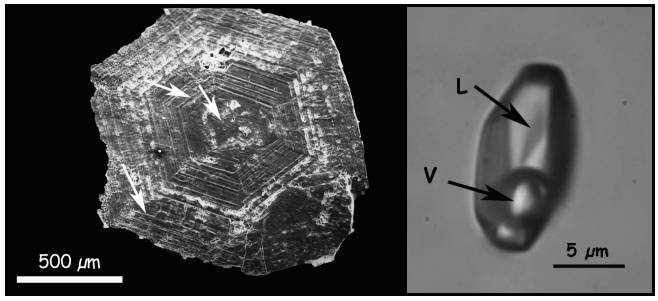

Ph.D. Supervisor,
Univ. Prof. Dr. Corina Ionescu

Ph.D. Student,
Ágnes Gál

Cluj-Napoca
2014

Table of contents

Chapter 1. Introduction

The Apuseni Mountains (AM) where mining is documented back in past for millenia, comprise some of the classical world-class ore deposits of Europe. The vein- and porphyry-type Au-Ag and minor Pb-Zn mineral deposits genetically related to the Neogene magmatism mostly occur within the so-called "Gold quadrangle". Despite the centuries-long geological investigations and mining, the genesis of these ore deposits is not yet fully understood. In particular, modern analytical tools were used only in a few studies. The Au mineral deposit at Certej is one of the cases poorly investigated using modern research methods. The aim of this study is to unveil the specific genetic processes leading to the formation of the Certej intermediate sulphidation type epithermal Au-rich ore deposit associated to the Neogene 'Băiaga' andesite with particular emphasis on the investigation of hydrothermal quartz crystals and the hydrothermal alteration products related to the mineralizing processes.

Chapter 2. Research history

Some of the well-known and very rich ore deposits of the Southern Apuseni Mountains, such as Roşia Montană, Abrud and Ruda-Barza, were mined by the Romans. The deposits at Săcărâmb, Zlatna, Abrud, Brad and Hondol were mined during the XVIII-XIXth centuries. Detailed research was done by Fichtel (1780), Herbich (1873), Ackner (1855), von Hingenau (1857), Inkey (1885), Koch (1885) and Primics (1888).

Ghiţulescu & Socolescu (1941) pioneered a complex stratigraphic, tectonic, magmatic and metallogenic investigation of the Southern Apuseni Mountains based on geological and geophysical methods. The investigation by Udubaşa et al. (1979) in the southern part of the Brad-Săcărâmb area revealed the morphological and paragenetical-geochemical diversity of the mineralization. Telluride minerals occurring in the Certej area were subjected to more analytical investigations, and the results were published by Ioan et al. (1993), Şimon et al. (1994, 1995), Cioflică et al. (1992, 1996), Udubaşa et al. (1993), and Cook & Ciobanu (2004). Alderton & Fallick (2000) described the nature and genesis of the Au-Ag-Te mineralization from the Săcărâmb, Măgura, Băiaga-Hondol and Bocşa deposits. New geological data along with a new mineralization model of the Certej ore deposit were published by Pricopie et al. (2004). Apopei et al. (2012) mention the presence of ferricopiapite, coquimbite and epsomite and Apopei et al. (2014) the presence of hessite, petzite and stützite in the Certej ore deposit.

The exploration data obtained by DevaGold Company resulted in a renewed economical perspective for the Certej ore deposit.

Chapter 3. Geological setting

The Apuseni Mountains (AM) (Fig. 3.1) belong to the Carpathian-Pannonian Region (CPR), together with the Pannonian Basin and the Transylvanian Basin.

Based on geochemical and radiometric age data, Pécskay et al. (1995, 2006), Seghedi et al. (2004) and Harangi & Lenkey (2007) presented a classification of the Neogene magmatic rocks in the CPR. They distinguished the following groups:

- Felsic calc-alkaline series of Miocene age (21–13 Ma);
- Intermediate calc-alkaline series of Middle Miocene-Quaternary age (16.5–2 Ma);
- K-alkaline and ultra-alkaline series of Middle Miocene-Quaternary age (15–0.02 Ma);
- Na-alkaline series of Late Miocene-Quaternary age (11–0.2 Ma).

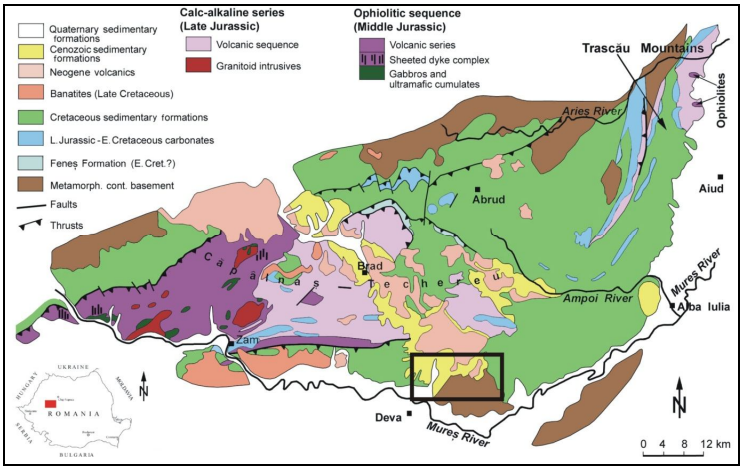

Fig. 3.1. Simplified geological map of the Southern Apuseni Mountains (from Ionescu & Hoeck, 2010; redrawn and modified after Saccani et al., 2001). The bottom left insert shows the position of the map within Romania. The rectangle marks the study area within the SAM.

The Neogene magmatic formations in the Southern Apuseni Mountains (SAM) show various volcanic and intrusive features: composite volcanoes, volcanic necks, lava flows, subvolcanic bodies and volcaniclastic sequences. Most of the rocks occur along a general NW-SE oriented structural trend which follows the orientation of the extensional basins formed along the western part of the AM. However, a second structural trend oriented NNE-SSE can also be identified. According to Roşu et al. (1997; 2004), four distinct areas of Neogene magmatic rock occurrences can be distinguished: (a) Baia de Arieş–Roşia Montană–Bucium, (b) Zărand–Brad–Zlatna, (c) Săcărâmb, and (d) Deva (including also the Uroiu shoshonite body).

The trace element contents and stable isotope ratios of the Apuseni Mountains magmas are clearly related to island arc type subduction processes. LILE, LREE, Pb and Sr enrichment along with Nb-Ta depletion and Pb, Sr and Nd heavy isotope depletion are the geochemical features suggesting a subduction-related metasomatism of the mantle lithosphere (Harris et al., 2013).

Block rotation-related extensional tectonics was probably the triggering impetus of the magma generation during Miocene (Harris et al., 2013). Seismic mantle tomography imaging suggests the presence in depth of a high-velocity body, interpreted by Harris et al. (2013) as a relic of a subducted oceanic crust beneath the Apuseni Mountains.

Three main mineralization types can be distinguished in the Apuseni Mountains (Ciobanu et al., 2004):

- Epithermal gold vein systems crosscutting the pre-volcanic basement and the Neogene lavas and intrusions, as well as the Cretaceous and Neogene sedimentary rocks. Examples of mineral deposits of this type are Ruda-Barza, Brădişor and Musariu (Milu et al., 2003; Cook et al., 2005);
- Porphyry type Cu-Au mineralizations generated in Late Miocene. They represent disseminated ore minerals in subvolcanic intrusive rocks and show stockwork structures (Berbeleac et al., 1995). The ore deposits at Deva, Roşia Poieni, Valea Morii and Rovina belong to this type;
- Breccia-related gold mineralizations such as Roşia Montană (Leary et al., 2004), Bucium, Rodu-Frasin and Baia de Arieş.

Chapter 4. Geology of the Certej area

In the close neighborhood of the Certej ore deposit, sedimentary rocks of Cretaceous and Neogene age occur. The former are quartzitic sandstones, mudstones, calcareous mudstones (marls), microconglomerates and black shales. The Neogene conglomerates, sandstones and calcareous mudstones display an overall plastic behavior.

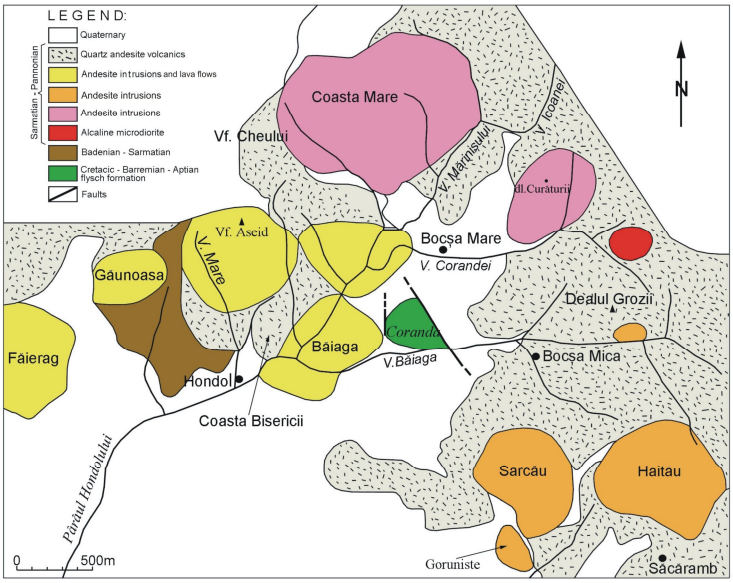

Fig. 4.1. Simplified geological map of the Certej area (modified, from Udubaşa et al., 1979) showing the main Neogene volcanic bodies and sedimentary formations in the Hondol-Bocsa Mica-Săcărâmb area.

The magmatic activity in the Certej area is assigned to two distinct phases (Pricopie et al., 2004). During the first phase, the intrusion of andesitic magmas which generated the 'Hondol andesite' and the 'Dealul Grozii andesite' took place. The intrusion-related breccias contain Au- and Ag-rich minerals in a hydrothermal mineral association deposited along a system of NW-SE and NE-SW trending fractures. In the second magmatic phase, the 'Băiaga andesite' was emplaced, causing deformation, brecciation and thermal transformation of the host Cretaceous and Neogene sedimentary rocks (Pricopie et al., 2004). Upon cooling, the hydrothermal fluids emanated by the intrusive body lead to the intense hydrothermal transformation of both the magmatic and the sedimentary rocks and to Au-Ag mineralizing processes. The mineralizing hydrothermal system was mainly controlled by the NW-SE and NE-SW striking faults (Pricopie et al., 2004). The surrounding Cretaceous and Neogene sediments acted as an environment that, due to specific physical, chemical and mineralogical characteristics, was prone to be mineralized.

The main ore minerals found in the Certej mineral deposit (Udubaşa et al., 1979, 1992) are: pyrite (to which most recoverable gold content is linked), marcasite (Au-bearing), pyrrhotite (Au-bearing), Cd-rich sphalerite, greenockite, Ag-rich galena, chalcopyrite, tetrahedrite-tennantite, arsenopyrite (Au-bearing), bournonite, boulangerite, meneghinite, stibnite, mackinawite, native gold, 'electrum' (Ag-rich variety of gold) and tellurides (kostovite).

Chapter 5. General data on quartz

In the 0–12 GPa pressure and 0–2,800 ºC temperature domain, the following SiO_2 phases can be present: α-quartz$^{(trigonal)}$ (low-T quartz) and β-quartz$^{(hexagonal)}$ (high/T quartz), tridymite$^{(triclinic)}$, cristobalite$^{(tetragonal)}$, coesite$^{(monoclinic)}$, stishovite$^{(tetragonal)}$ and a liquid (melt) phase (Swamy et al., 1994). β-quartz, tridymite, cristobalite, coesite and stishovite are metastable at Earth surface conditions (Deer et al., 2003). Other metastable SiO_2 phases at near-surface conditions are the 'amorphous' or partially 'amorphous' opal-CT, opal-C, and moganite.

The experiments on artificial quartz growth (Hosaka, 1995) show that prismatic habit mostly develops in hydrothermal conditions, while at high temperature hexagonal pyramid is the characteristic form. Kawasaki (1995) found that quartz morphology may change significantly with increasing Al content of the solutions. Quartz easily retains the entrapped fluids (e.g., H_2O, CO_2, NaCl, CO, H_2O, NaCl, CH_4, NH_4, Cl^-, NO_3^-, HCO_3^- and SO_4^{2-}), as well as various solid mineral phases (e.g., rutile, tourmaline, amphibole and micas). Quartz forms twins according to the *c*-axis. The most frequent are Dauphiné and Brazil twinning, respectively.

Traces of B, Mg, Na, P, Cl, K, Ti, Mn, Fe, Ge, Sn, Al, Li, Ti, Al, Na, Fe, Au, Ag, P were identified in magmatic, metamorphic and hydrothermal quartz. The most variable is the Al content and it generally correlates with Li. The trace element concentration significantly depends on formation temperatures (Gubareva, 1999; Allan & Yardley, 2007). Out of the above mentioned trace elements, only a few can

replace Si atoms in the crystal lattice in tetrahedral position: Al^{3+} (0.51 Å), Ga^{3+} (0.62 Å), Fe^{3+} (0.64 Å), Ge^{4+} (0.53 Å), Ti^{4+} (0.64 Å) and P^{5+} (0.35 Å) (Götze et al., 2001). In case of some of the replacing elements (e.g. Al^{3+} and Fe^{3+}) the resulting charge imbalance requires other cations, such as H^{+}, Li^{+}, Na^{+}, K^{+}, Cu^{+}, Ag^{+}, to be included in the structure of quartz and placed in inter-lattice positions (Götze et al., 2001). According to Götze et al. (2004) quartz of different genesis admits particular trace elements (Al, Ti, Ge, Na, K and Li) in specific concentration range. In some vein quartz related to hydrothermal Au deposits trace element anomalies have been recorded: Al >50 ppm and Sr >0.6 ppm (Monecke et al., 2002).

Relationships between Al content and morphological features of artificially grown quartz crystals have been studied by Kawasaki (1995, 2003). Where Al incorporations are present, a morphological step appears in the lattice. Al occurs in the quartz lattice at high growth rates (Allan & Yardley, 2007). Allan & Yardley (2007) demonstrated that magmatic and volcanic quartz grows faster than the hydrothermal quartz.

Chapter 6. Samples and analythical methods

The work strategy involved a methodology adapted to the aim of the study and covered a complex approach ranging from field observation and sampling to laboratory investigation with various instrumental analytical techniques. The investigation methods used in this study are listed in Table 6.1.

Table 6.1. Investigation methods and data processing tools used in the study.

Investigation Method	Sample/analyses quantity
1. Field work	586 samples, 341 observation points
1a. Structural measurements in the field	124 positions of structural elements
1b. Macroscopic observations	316 samples
2. Polarized light optical microscopy (transmitted, reflected light) (OM)	167 thin sections, 22 polished sections
3. X-ray powder diffraction (XRPD)	50 samples, 70 diffractograms
4. Goniometry	210 quartz crystals
5. Cathodoluminescence (CL)	20 quartz crystal samples
6. Quartz twinning	47 samples
7. Optical emission spectroscopy (OES)	7 quartz crystal samples
8. Neutron activation analyses (NAA)	7 quartz crystal samples
9. Microthermometry	18 samples, 489 measurements
10. Electron microprobe analysis (EMPA)	24 samples, 164 point analyses
11. Raman spectroscopy	39 samples, 30 fluid inclusions
12. K-Ar radiometric dating	3 samples
13. Computed data processing	10 programs

Chapter 7. Field observations

The lower levels and the western side of the Coranda open pit expose the Băiaga intrusive magmatic body (Fig. 7.1). The Cretaceous (Barremian-Aptian) flysch-facies sedimentary rocks (black shales, sandstones, conglomerates, breccias) crop out in the central part of the open pit, whereas the Neogene (Miocene) sandstones and marls occur in the uppermost levels of the eastern side of the quarry.

Fig. 7.1. The geological formations exposed in the Coranda open-pit: Băiaga andesite, Cretaceous and Neogene sediments.

Chapter 8. Structural analysis

Fissures/fractures, other than cooling joints, are present in both the intrusion and the host rocks. Sealed fissures (veins), 0.3–2.5 cm wide, characterize mostly the Cretaceous host rocks. The planar structural elements were grouped into three categories.

Brittle deformation in the host rocks. Two planar elements have been recorded (M1 and M2). M1 is subvertical and has a NW-SE oriented dominant strike. The second one (M2) corresponds to another shear fracture/fissures pole forming a dihedral angle of 30° with the first one. This configuration reflects sinistral strike-slip movement, with main shear-plane dipping NE (Fig 8.1).

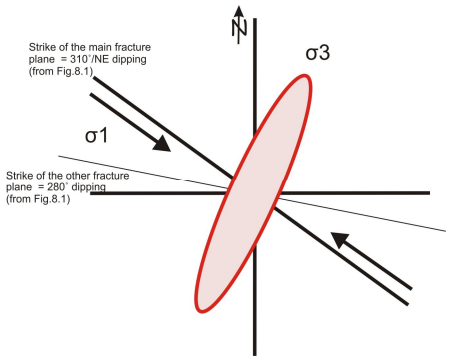

Fig. 8.1. Deformation ellipsoid and corresponding stress axes σ1 and σ3 in the host rocks (Coranda open pit).

Brittle deformation in the contact zone of the intrusive body. The main subvertical shear plane can be inferred as striking NW-SE and dipping NE, similar to that pointed out for the host rocks. The other recorded planar elements represent WNW-ward dipping fracture planes, which probably were rotated during sinistral shearing.

Fissure system of the intrusive body. The planar elements (cooling joints) suggest three main cooling-cracking directions (mainly cross- and steep diagonal-joints), located at acute angles. The most prominent of them defines a subvertical (88°-90°) plane with NW-SE striking steeply dipping longitudinal joints identical with those identified in both the host rocks and the contact zone of the intrusion. A second plane corresponds to diagonal joint planes striking NE-SW, while the third one represents ENE-WSW striking joints. These three joint planes most likely belong to the same unique jointing system related to the intrusive body, developed normal to the main (subhorizontal) cooling surface.

Chapter 9. Optical microscopy

The main rock types in the study area (Băiaga andesite, Cretaceous flysch rocks and Neogene sandstones), revealed both primary and secondary features.

The **Băiaga andesite** is composed of plagioclase, amphibole, clinopyroxene and rare quartz phenocrysts in a microcrystalline groundmass. Apatite and magnetite occur as accessory minerals. Despite that the phenocrystals and the groundmass are almost entirely altered into illite, fine-grained muscovite ('sericite'), opaque minerals, K-feldspar ('adularia') and calcite, the 'ghost' porphyritic texture is still recognizeable (Fig. 9.1).

The **Cretaceous sandstones** are mostly of quartz-arenitic type but carbonate-cemented, feldspar-bearing, muscovite-bearing and feldspar-bearing types are also present. A large variety of mineralogical aspects of hydrothermal transformation types can be seen in sandstones: sericitic (phyllic) alteration, silicic alteration, carbonatation (Fig. 9.2), K-feldspar alteration ("adularization") and pyritization.

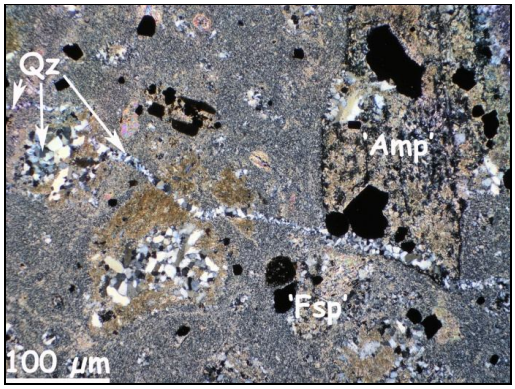

Fig. 9.1. Polarized light microphoto of alteration products in the Băiaga andesite (sample CRTJ_176).
'Ghost' porphyritic texture, with recognizeable amphibole (Amp) and feldspar (Fsp) phenocryst shapes. Opaque minerals are black in the image. P+.

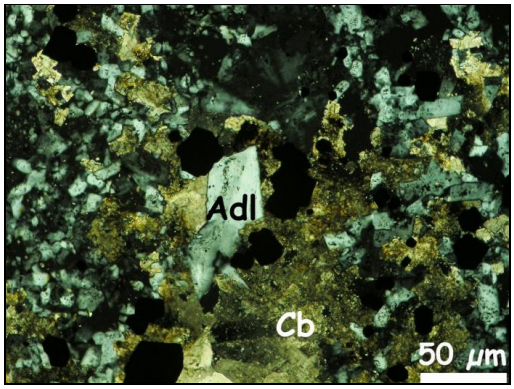

Fig. 9.2. Polarized light microphoto showing idiomorphic adularia (Adl), carbonates (Cb) and opaque minerals in hydrothermally transformed sandstone (sample CRTJ_101). The large adularia crystal in center of photo is twinned. P+.

Thye **Cretaceous shales** reveal a laminated fabric consisting of alternating laminae of claystone and siltstone. The rock's black colour is due to organic matter. Quartz, clay minerals, muscovite and calcite are the main primary mineralogical components of siltstone laminae while opaque mineral grains (pyrite?), sometimes associated with quartz and calcite, adularia and aboundant sericite were formed by hydrothermal transformation processes.

The **Neogene sandstones** are coarse-grained and quartz-rich arenites, carbonate-cemented (bazal type). Sericite (illite?) and rarely pyrite were observed in places. The main differences between the Neogene and Cretaceous sandstones consist in the coarser grain size of the former and more frequent pyrite in the latter.

A number of ore minerals were identified by reflected light optical microscopy: pyrite (Fig 9.3), sphalerite (Fig. 9.4), galena (Fig. 9.4), tetrahedrite and bournonite (Fig. 9.4).

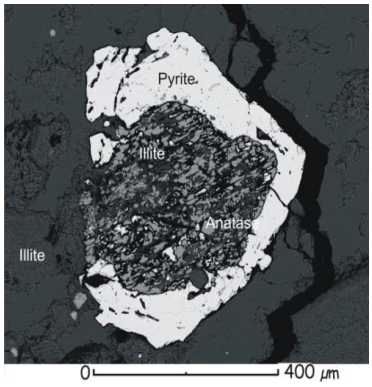

Fig. 9.3. Backscattered electron (BSE) image of illite aggregate (with an anatase grain) overgrown by pyrite (Py). Sample CRTJ_173.

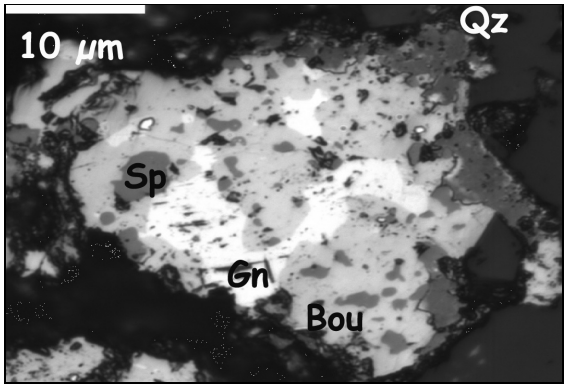

Fig. 9.4. Microphoto of various ore minerals: sphalerite (Sp), galena (Gn), bournonite (Bou) in quartz (Qz). Sample CRTJ_173. Polarized, reflected light; 1P.

Chapter 10. X-Ray powder diffraction (XRPD)

A number of minerals, in particular in the mineralized areas, were identified by XRPD. They range from sulfides (pyrite, Fig. 10.1), oxides (anatase, magnetite, and quartz, Fig. 10.1) hydroxides (goethite and gibbsite), carbonates (calcite), sulphates (barite, voltaite, gypsum, alunogen, alunite, jarosite - Fig. 10.1 - and hydroniumjarosite) to silicates (kaolinite, halloysite, muscovite - Fig. 10.1 - , tobelite - Fig. 10.1 - illite, illite/smectite, clinochlore, orthoclase, sanidine, and microcline). An amorphous phase (~7–20%) was also detected in most of the samples.

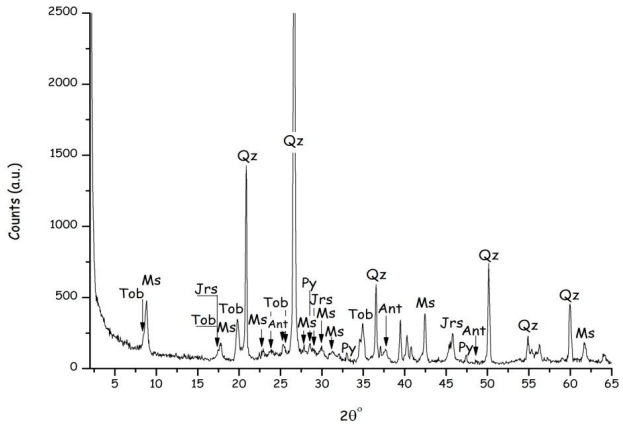

Fig. 10.1. X-ray diffractogram of a hydrothermal assemblage in Băiaga andesite, with quartz (Qz), muscovite (Ms), hydroniumjarosite (Jrs), tobelite (Tob), anatase (Ant) and pyrite (Py). The lump in the pattern between ~22 and ~33 º2θ is due to the 'amorphous' phase (sample CRTJ_178).

Chapter 11. Morphological and crystallographical study of hydrothermal quartz

In the Certej mineral deposit, hydrothermal quartz crystals are found in vugs and voids, veins and breccias. They often form monomineralic aggregates in veins but might be accompanied by calcite, K-feldspar, barite and sulphides. Large idiomorphic crystals (Fig. 11.1) occur in geodes with no other accompanying minerals. The quartz crystals show mostly long-prismatic habit. Macroscopic features include „sceptre quartz" and negative „sceptre quartz" form, as well as crystals transversally striated on the prism faces. In all cases, one of the rhombohedral faces is more developed than the other two.

Fig. 11.1. Typical appearance of large idiomorphic hydrothermal quartz crystals at Certej, with turbid root (right) and transparent crystal end (left). Length of the crystal is 5.2 cm (sample CRTJ_72).

The quartz crystals from the Certej ore deposit are colourless. Their clarity varies from transparent (water-clear) to translucent („spider-net"-like) or almost opaque (turbid, milky-white) (Fig. 11.1). Sometimes the quartz crystals display a turbid core surrounded by a transparent outer rim or a turbid root associated with a transparent crystal top. Such appearance is characteristic for quartz crystallized in epithermal conditions (Van den Kerkhof & Hein, 2001) and is due to abundant fluid inclusions.

The crystal forms identified on hydrothermal quartz in Certej are (Fig. 11.2): prism *m* $(10\bar{1}0)$, positive (r) and negative (z) rhombohedron $(10\bar{1}1)$, higher-index rhombohedron faces {(h.0.$\bar{h}$.l), (l $(20\bar{2}1)$, 'l $(02\bar{2}1)$, M $(30\bar{3}1)$, 'M $(03\bar{3}1)$, γ $(40\bar{4}1)$, 'γ $(04\bar{4}1)$, ξ $(60\bar{6}1)$, 'ξ $(06\bar{6}1)$, φ $(70\bar{7}1)$, 'φ $(07\bar{7}1)$, Ψ $(110\bar{1}11)$, Ψ $(011\bar{1}11)$}. The higher-index rhombohedral faces appear grouped, forming step-like features.

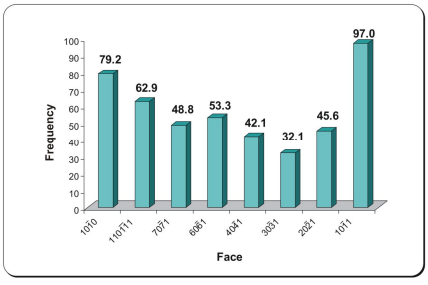

Fig. 11.2. Average frequency of main crystal faces of quartz at Certej.

All mentioned crystal forms were identified at all mine levels but with variable percentages, ranging from 100% (*m, r, z*) to 14.5 % (*M*). Distribution of the $\{10\bar{1}1\}$ faces appears to be constant in the whole mining depth range and shows the highest frequency among all faces. The frequency of the $\{110\bar{1}11\}$ and $\{70\bar{7}1\}$ faces significantly increases with decreasing depths whereas the $\{20\bar{2}1\}$ and $\{10\bar{1}0\}$ faces are more frequent upwards. The faces $\{40\bar{4}1\}$ and $\{30\bar{3}1\}$ show a slight decrease in frequency from lower to upper levels of the ore deposit.

Cathodluminescence

The hydrothermal quartz crystals studied show weak light blue to brown luminescence. Zoning was observed in all samples. The investigated quartz crystals have Al contents above detection limits whereas Ti and Fe are below detection limits. Since the results are beyond required analytical accuracy (i.e. Ti and Fe content at a few ppm level), it remains unclear which of the two elements is responsible, besides Al, for the observed CL zoning in the Certej hydrothermal quartz crystals. However, it is more likely that Al is the element which plays the major role.

Twinning

The etched surface of the cut crystals shows several combinations of twinning types. The most characteristic combinations are D1b (dominant Dauphiné twinning combined with subordinate Brazil twinning) and D2B oberved only at the crystal margins where dominant Brazil twinning is present (Fig. 11.3). The statistical processing of results indicates BD1 and BD0, as the most frequent twinning combinations and Brazil twinning as the most widespread (present in all combinations) twinning type.

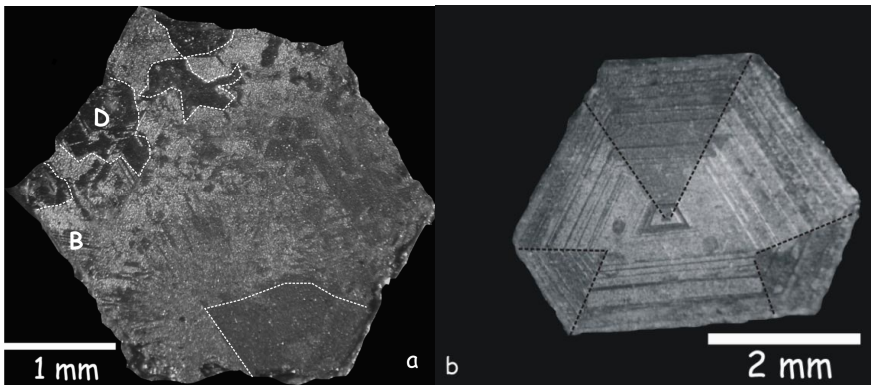

Fig. 11.3. Etched surfaces of quartz slices perpendicular to the *c*-axis showing zoning and combination of Dauphiné and Brazil twins (**a**) and Brazil twins (**b**) (marked by dashed lines).

Chapter 12. Optical emission spectroscopy

The following trace components were identified by OES in the hydrothermal quartz crystals at Certej: Al_2O_3, CaO, Fe_2O_3, MgO, Mn, Cu, Ag, Ba, Pb and Ti. No systematic variation in the concentration of the analyzed elements could be detected in function of mining levels.

Chapter 13. Neutron-activation analyses

The Certej hydrothermal quartz crsytals contain Cs, Ba, Ce, Nd, Sm, Eu, Yb, As, Sb, Sc, Ta, Cr, Mn, Au, Zn and Hg. Compared with the upper continental crust composition (data from Rudnick & Gao, 2003), Certej quartz shows significant enrichment for several elements. Sb and Au display strong positive anomalies. Na, K, Ba, Sm, Eu have higher concentration at Certej as compared to hydrothermal quartz in other epithermal ore deposits (e.g. Monecke et al., 2002). If compared with trace element distribution in the Neogene magmatic rocks of the Apuseni Mountains (Roşu et al., 2004) and with that of a sandstone (Götze, 1998), the Certej hydrothermal quartz shows enrichment only in Lu. Sb displays some variation with depth. As, a (semi)volatile element, concentrates at higher levels of the hydrothermal system where it was effectivey entrapped in the growing quartz crystals. Similarly, other volatiles such as As and Hg, show highest concentrations at the most elevated open pit levels.

Chapter 14. Fluid inclusion studies

In all studied Certej samples the „spider net structure" characteristic for epithermal quartz crystals (Van den Kerkhof & Hein, 2001) was found. Primary, secondary and pseudo-secondary fluid inclusions were identified. Most of the observations and measurements were performed on primary fluid inclusions, but some secondary inclusions were also studied.

Morphology of the fluid inclusions is variable, ranging from irregular to elongated-prismatic and isometric. Many primary inclusions display negative crystals. Fluid inclusion size is also variable, ranging from 2 µm up to 200 µm in some cases (Fig. 14.1). In all samples the L-type and V-type fluid inclusions are located along the same crystal growth zone or along the same fissure, forming the so-called "fluid inclusion assemblage" (FIA) (Goldstein & Reynolds, 1994) (Fig. 14.1).

In the honey-yellow coloured zones of sphalerite, fluid inclusions can also be found. Thery are generally smaller (<10 µm) as compared with those found in the hydrothermal quartz crystals. Their shape varies from regular (negative crystal) to irregular. Both primary and secondary inclusions were observed.

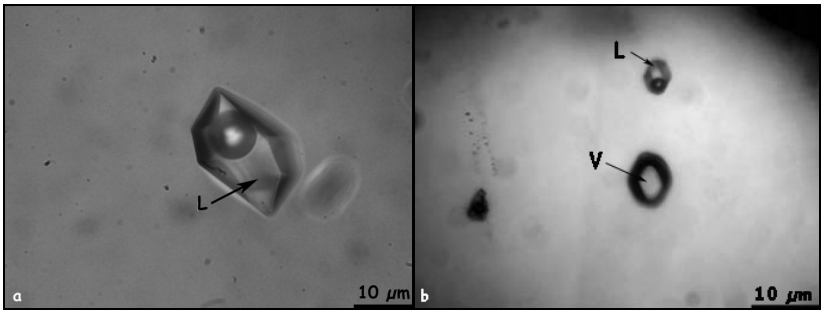

Fig. 14.1. **a)** L-type primary fluid inclusion with perfect negative crystal shape; **b)** Fluid inclusion assemblage, with contemporaneous fluid-rich inclusion (L) and gas-rich (V) inclusions. Transmitted polarized light, 1P.

The homogenization temperature (Th) ranges from 179 to 317 °C (Fig. 14.2 and 14.3). The last ice-melting temperature varies between -0.1 and -3.3 °C, while first ice melting temperature fits in the -19.3 to -22.2 °C interval (Table 14.1). The minimal entrapment temperature (Te) of fluid inclusions ranges between 179 and 317 °C. The first ice melting temperatures suggest a H_2O-NaCl dominant system, with $CaCl_2$, $MgCl_2$ or KCl content (Bodnar & Vityk, 1994).

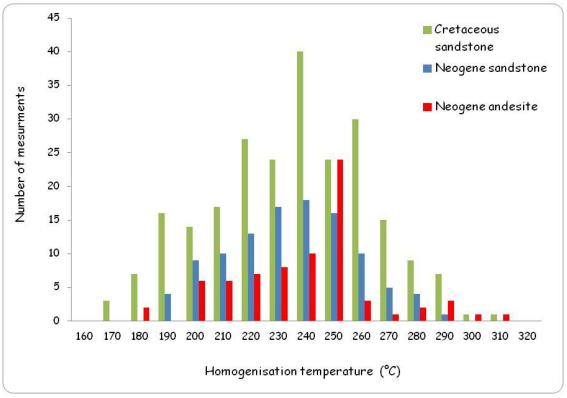

Fig. 14.2. Statistical distribution of homogenization temperature in quartz crystals in function of host-rock: Cretaceous flysch rocks (n = 227), Neogene sandstone (n = 98) and Neogene andesite (n = 75).

The last ice melting temperature (Tm_{ice}) values (calculated according to Steele-McInnis et al., 2012) indicate a salinity of hydrothermal solutions in the range of 0.18-5.41 mass% $NaCl_{eq.}$

The hydrotermal quartz was sampled along a vertical elevation of 170 m, covering sevenmining levels, from the Coranda open pit to underground (Fig. 14.4).

Fig. 14.3. Distribution of last ice melting temperature vs. homogenization temperatures in quartz crystals of the Certej ore deposit according to host-rock types: Cretaceous flysch rocks (n=227), Neogene sandstones (n=98) and Neogene andesites (n=75).

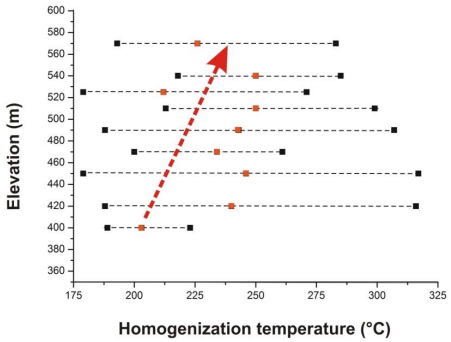

Fig. 14.4. Variation of fluid inclusion homogenization temperatures (n=409) in quartz crystals with elevation (mining levels). Red squares are average values and the dashed lined arrow indicates the general variation trend.

Table 14.1. Results of microthermometric investigation of fluid inclusions at Certej. Abbreviations: fl - Cretaceous black flysch rocks, sands - Neogene sandstones, and - Neogene andesites; sph – sphalerite. n – number of measurements). n_{total} = 489.

Elevation (m a.s.l.)	Sample no.	Host mineral	Rock-type	n	Temperature (°C)			Salinity mass% $NaCl_{eq.}$	Pressure (bar)	Density (g/cm^3)
					Th	Tm_{ice}	T_e			
575	CRTJ_170	quartz	sands	33	193-266	-2.2 to -0.3		0.53-3.71	13.05-55.98	0.74-0.9
540	CRTJ_341	quartz	sands	10	164 302	-1.1 to -0.1		0.18-1.91	6.82-87.68	0.70-0.92
533	CRTJ_91	quartz	sands	20	218-285	-1.6 to -0.6		1.05-0.74	27.6-57.8	0.78-0.83
526	CRTJ_113	quartz	fl	29	179-271	-1.7 to -0.7	-21.9 to -19.3	1.22-2.90	9.59-54.59	0.78-0.90
525	CRTJ_340	quartz	sands	10	211-317	-2.0 to -0.4		0.70-3.39	19.39-107.8	0.68-0.86
525	CRTJ_339	quartz	sands	15	190-321	-2.4 to -0.2		0.35-4.03	12.29-115.18	0.67-0.91
513	CRTJ_32	quartz	sands	32	213-299	-1.0 to -0.5		0.88-1.74	27.13-64.63	0.76-0.84
494	CRTJ_72	quartz	fl	50	196-299	-2.4 to -0.2		0.35-4.03	19.78-128.10	0.65-0.86
490.3	CRTJ_317	quartz	fl	42	190–307	-3.3 to -0.1	-22.2 to -19.6	0.18-5.41	12.36-135.3	0.63-0.91
490.3	CRTJ_318	quartz	fl	25	227-297	-2.1 to -0.5		0.88-3.55	28.03-82.16	0.72-0.83
490.3	CRTJ_320	quartz	and.	36	188-273	-1.8 to -0.2		0.35-3.06	11.85-57.12	0.76-0.89
489	CRTJ_173	quartz	sands	25	232 - 277	-1.6 to -1.2		2.07-2.74	43.62-45.51	0.8-0.81
473	CRTJ_51	quartz	fl	24	200–261	-2.2 to -0.5		0.88-3.71	18.54-33	0.82-0.86
450	CRTJ_312	quartz	fl	22	185-289	-1.8 to -0.1		0.18-3.06	11.11-72.89	0.72-0.89
450	CRTJ_314	quartz	fl	15	206-279	-1.2 to -0.4		0.70-2.07	17.38-62.81	0.75-0.87
450	CRTJ_315	quartz	and	47	179-317	-2.3 to 0.1		0.18-3.87	9.72-122.96	0.66-0.90
420	CRTJ_328	sph	and	47	188-316	-3.3 to -0.2	-22.2 to -21.5	0.35-5.41	17.24-72.31	0.77-0.90
403.7	CRTJ_296	quartz	and	7	171-223	-0.7 to -0.5		0.88-1.22	7.97-24.06	0.84-0.91

Chapter 15. Raman spectroscopy

Raman spectroscopy investigations were performed on mineral associations as well as on fluid inclusions from quartz crystals and from sphalerite.

The Raman-spectroscopical investigation resulted in the determination of numerous mineral phases of small size or as inclusions: anatase, sphalerite, pyrite, magnetite, hematite, bournonite, jamesonite, alabandine, tetrahedrite, calcite, barite, muscovite, quartz. The minerals identified in the samples only by Raman spectroscopy are: hematite, bournonite and jamesonite.

The following chemical compounds, characterized by specific Raman-active vibrations, have been identified in the fluid inclusions from quartz crystals: CO_2 (double picks at ~1284 cm^{-1} and at ~1387 cm^{-1}, respectively), CH_4 (~2918 cm^{-1}), N_2 (~2331 cm^{-1}), H_2S (~2611 cm^{-1}), water-soluble H_2S (~2590 cm^{-1}), CO (~2143 cm^{-1}) and H_2O (1600 cm^{-1}2900 $cm^{-1}$and 3750 cm^{-1}) (Fig. 15.1).

The composition of the entrapped fluid as recorded at room temperature strongly differs from that recorded at the homogenization temperature. At room temperature, the CO_2 concentration is between 4.97 and 95.55 mol%, and H_2O concentration between 0 and 94.41 mol% (Table 15.1). Contrary, the homogenized fluid contains 0–29.75 mol% CO_2 and 67.00–99.98 mol% H_2O. These large differences indicate a high variability of the homogenized composition and point to a heterogenous entrapping of the fluids in the growing quartz crystals. Nevertheless, the fluid inclusions contain also phases which are not Raman-active, such as NaCl and/or $CaCl_2$.

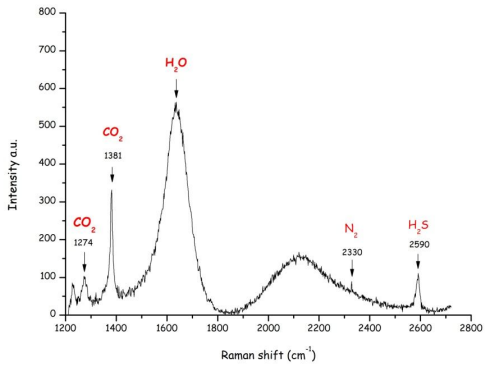

Fig. 15.1. Raman spectrum showing the presence of CO_2, H_2O, N_2 and H_2S molecules in the fluid inclusions of hydrothermal quartz in Certej (sample CRTJ_32) at room temperature (22 °C).

Table 15.1. Concentration of Raman-active components (in mol%) in the fluid inclusions in quartz crystals as recorded at room temperature and at the homogenization temperature.

Component	Fluid composition at room temperature	Fluid composition at T_h
CO_2	4.97–95.55	0.00–29.75
CH_4	0.00–1.20	0.00–0.27
N_2	0.00–11.19	0.00–7.24
H_2S	0.00–5.55	0.00–3.14
H_2O	0.00–94.41	67.00–99.98

Chapter 16. Electron microprobe analysis

The results of electron microprobe analyses for ore and gangue minerals in the Certej area are given in Table 16.1. From the native elements, silver and tellurium were identified by means of energy-dispersive (ED) spectra. Sulphides and sulphosalts identified at Certej include pyrite, sphalerite, galena, chalcopyrite, arsenopyrite, stibnite, tennantite-tetrahedrite series minerals, bournonite, gersdorffite. Tellurides are unusually rich in mineral species: hessite, petzite, altaite, coloradoite, nagyágite, sylvanite, stützite, melonite (Figs. 16.1 and 16.2; Table 16.2). Anatas and tellurite represent the oxides. Carbonates, sulphides (gypsum, barite and jarosite) and aluminium phosphate-sulphate minerals (APS) are also found. K-feldspar, illite and kaolinite were identified as silicate minerals.

Table 16.1. Samples analyzed by microprobe from the Certej ore deposit. APS = aluminium-phosphate-sulphate minerals.

Depth of sampling (m a.s.l.)	Identified minerals
575	pyrite, anatase, quartz, jarosite, K-feldspar, illite
566	pyrite, anatase, quartz, jarosite, K-feldspar, illite
566	pyrite, anatase, quartz, barite, illite
562	pyrite, sphalerite, galena, barite, illite
562	pyrite, sphalerite, galena, stibnite
542	sphalerite, unidentified sulphosalt with Cu-Pb-Sb-S
534	sphalerite, tetrahedrite, quartz, calcite
533	sphalerite, galena, quartz, APS, K-feldspar, illite
532	pyrite, anatase, APS, K-feldspar, illite
526	pyrite, sphalerite, galena, chalcopyrite, sylvanite/krennerite, anatase, quartz, gypsum, APS, calcite, K-feldspar, kaolinite
494	pyrite, sphalerite, galena, barite, epidote, K-feldspar
494	silver, tellurium, pyrite, splaerite, gersdorffite, hessite, sylvanite, melonite, anatase, barite, APS, K-feldspar, illite (fig 1
492	pyrite, sphalerite, galena, stibnite, unidentified phase with As-Sb-Cu-Pb-S, unidentified phase with Cu-Sb-S, quartz, anatase, illite
490	Pyrite, galena, quartz, rhodochrosite
490	pyrite, sphalerite, tennantite-tertahedrite, quartz, anatase, rhodochrosite, K-feldspar
487	pyrite, Ag-Te, anatase, K-feldspar, illite
481	pyrite, sphalerite, unidentified phase with Cu-Sb-S, unidentified phase with Cu-Sb-Ag-S, albite, K-feldspar
476	tellurium, silver, pyrite, sphalerite, unidentified phase with Cu-As-Sb-S, hessite, petzite, altaite, coloradoite, nagyágite, sylvanite/krennerite, stützite, melonite, tellurite, K-feldspar (fig 16.1)
473	pyrite, sphalerite, galena, chalcopyrite, hessite, dolomite
470	pyrite, sphalerite, galena, tetrahedrite, hessite
450	pyrite, sphalerite, chalcopyrite, bournonite, quartz, K-feldspar
403	pyrite, arsenopyrite, quartz

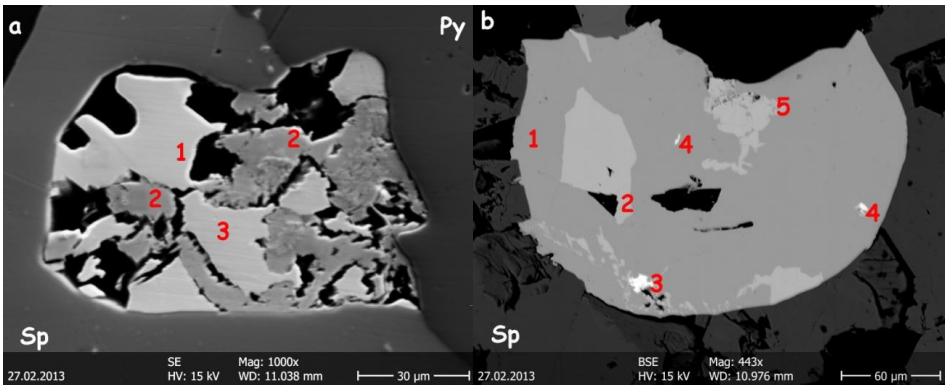

Fig. 16.1. Tellurides in sample CRTJ_100. **a)** SE image of hessite (1), tellurite (2) and stützite (3) in sphalerite (Sp); Py - pyrite; **b)** BSE image of hessite (1), petzite (2), coloradoite (3), altaite (4) and sylvanite (5) in in sphalerite (Sp).

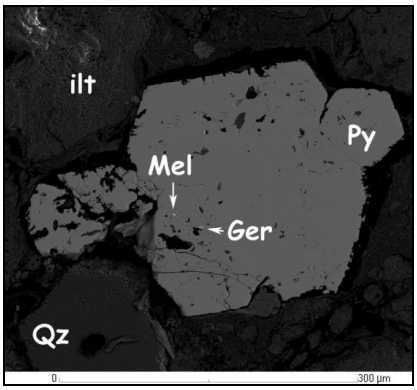

Table 16.2. Electron microprobe data (in mass%) for melonite in sample CRTJ_242.

Element	Content (mass%)
Ni	15.39
Te	79.05
S	2.1
Fe	3.45
Total	99.99

Fig. 16.2. BSE image showing inclusions of gersdorffite (Ger) and melonite (Mel) in pyrite (Py) in sample CRTJ_242. Other abbreviations: illite (ilt), quartz (Qz).

Chapter 17. K-Ar radiometric dating

The K-Ar ages obtained on illite and 'adularia' separates range between 11.86 ± 0.52 Ma and 12.29 ± 1.56 Ma. The radiometric ages obtained for the two K-bearing minerals (illite and 'adularia') are almost identical (taking into account the analytical errors). For this reason a K-Ar age of ~12 Ma for the hydrothermal activity at Certej can be considered as reliable.

Chapter 18. Discussions

Mineral deposits form as a consequence of interplay of various favorable factors. In the case of the Certej ore deposit a number of structural, lithological and geochemical conditions enabled metal concentration and deposition. In general, within a hydrothermal system a certain combination of several factors may lead to epithermal ore formation. Among these factors the most important are: the composition, temperature and pressure of the hydrothermal solutions, the host-rock type, the specific hydrothermal fluid-

host rock interaction (rock buffer, Giggenbach, 1984, 1997), and finally the fluid-rock equilibrium state (Robb, 2005).

Structural control. Three types of structural elements involved in ore formation at Certej and related to a) regional stress regime, b) internal effects of cooling of the intrusive magmatic body and c) intrusion-related deformation of the host-rocks, have been identified. The regional structural elements indicate extensional processes in the NE-SW direction. The local structural elements (expressed by quartz-, calcite- and pyrite-bearing veins within the host sedimentary rocks) allowed penetration and circulation of the mineralizing hydrothermal fluids. Each of the structural elements had a specific metallogenic role. Regional transtensional tectonics framed the intrusion of magma and emplacement of Băiaga andesite body and pre-determined the major directions of penetration as well as the circulation paths for the hydrothermal fluids within the host rocks. Intrusion-related host-rock deformation and brecciation were crucial for location and spatial limitation of the major mineralizing process. The role of the cooling joint system within the margins of the intrusive body itself remains unclear, but most likely it was minor if compared with the other two structural features mentioned above.

Genetic types of hydrothermal processes at Certej. Both the macroscopic and the microscopic observations point to alternating closed and open system conditions in which hydrothermal processes developed at Certej. Such conditions were favoured by the presence of the Cretaceous flysch host rocks, in particular the shales.

Products of both phyllic and potassic alteration are present at Certej. Consequently, the major chemical feature is a general K-metasomatism evolving from earlier potassic to later sericitic type upon general cooling. The hydrothermal assemblage also contains some minerals, such as kaolinite, illite, illite/smectite and halloysite, characteristic for the „intermediate argillic" type alteration (Gifkins et al., 2005). These minerals locally overprint earlier alteration products.

Intensity of hydrothermal process and fluid/rock ratio. The pervasive hydrothermal alteration of the Băiaga andesite and its encasing sedimentary rocks, as well as the ubiquitous K-metasomatic processes indicate intense circulation of hydrothermal fluids in the Certej area (see also Udubaşa et al., 1979; Alderton & Fallick, 2000). This suggests a high fluid-rock ratio which controlled the deposition of ore minerals.

Composition of the hydrothermal fluids

Information on hydrothermal fluid composition was obtained from NAA, fluid inclusion and Raman data for hydrothermal quartz crystals. The trace element content of hydrothermal quartz suggests the presence of the volatile/semivolatile elements such as As, Sb in the epithermal fluids.

Microscopic observation of fluid inclusions along with observations with the cooling-heating stages allowed the identification of a H_2O-NaCl system at the Certej ore deposit. Both gas-rich and liquid-rich

inclusions are present. The presence of CO_2, N_2, CH_4 and H_2S components in the epithermal system is supported by Raman studies.

The hydrothermal quartz crystals entrapped H_2O-rich fluids during their growth. The large variability of H_2O (67.00-99.98 mol%) and CO_2 (0.00–29.75 mol%) content in the homogenized fluid inclusions suggests that fast-growing individual quartz crystals formed in a boiling environment. Boiling of the hydrothermal fluid is also suggested by both liquid-rich and gas-rich inclusions of the same generation. Due to boiling, these components (gas and fluid) of the hydrothermal solution were entrapped in random proportions in fast-growing quartz crystals.

The wide interval of first ice melting temperatures (-19.3 to -22.2 °C) recorded at Certej, is difficult to interpret as each measured inclusion reflect a locally restricted situation. According to Bodnar & Vityk (1994) a H_2O-NaCl system has its eutectic at -21.2 °C, whereas the H_2O-NaCl-KCl system has an eutectic at -23.5 °C. The microthermometric data obtained so far point to an overall H_2O-NaCl type system, with some KCl component.

H_2O, CO_2, SO_2 and H_2S are the most common volatile components in hydrothermal systems (Einaudi et al., 2003). Quartz-hosted fluid inclusions at Certej additionally contain N_2 and CH_4. N_2 and CH_4 as well as CO_2 and H_2S could originate from the organic carbon-rich Cretaceous shales hosting the mineralization. These volatile components most likely played a major role in ore forming process at Certej acting as catalysing agents and regulators of metal transport and precipitation. The host rocks of mineralization at Certej are mainly Cretaceous black shales and sandstones with some organic content (e.g. carbon). Therefore, the CO_2, N_2, CH_4 and H_2S found in fluid inclusions in quartz can be interpreted as originating, at least partially, from the host rocks. The presence of H_2S (not necessarily of solely organic origin), for instance, could favour metal transport in the hydrothermal fluid, while the rest of the components do not form ligands with the ore-generating metals. They rather contributed to creation of favorable local conditions (e.g. reducing environment) for ore mineral deposition from the solutions.

Evolution of the hydrothermal fluids

Evidences from hydrothermal quartz characteristics

Quartz crystals showing ‘spider-net’ like core or lower part associated with water-clear periphery or crystal end indicate both the change of hydrothermal solution characteristics with time and a sequential crystal growth. The positive and negative „sceptre quartz” forms, the stripped prism faces and the higher-index rhombohedron also indicate the change in time of the parental hydrothermal solutions.

The intense zoning observed on the etched cut surfaces of hydrothermal quartz crystals suggests significant variation of the physical-chemical properties of the hydrothermal solution during the growth of quartz crystals. One of the variable parameters is the Al content. It is known that the replacement of Si^{4+} by Al^{3+} in quartz crystal lattice might cause strong structural deformation leading to local breaking of Si-O-Si bonds (Hashimoto, 2008). According to Sunagawa et al. (1999), the Brazil twinning occurs when Fe^{3+} ions

enters into the crystal lattice of quartz. Since the observations revealed the predominance of Brazil twinning, a significant role of Fe^{3+} replacement during crystal growth of quartz at Certej might be envisaged.

Subtle changes in quartz morphology and zoning features (e.g. alternation of stepping prism faces with rhombohedral faces), as well as the results of cathodoluminescence investigation probably reflect a chemical evolution (i.e. time-dependent changes) of the parent hydrothermal fluids.

Evidences from hydrothermal mineral assemblages and successions

Fluid composition changed with time as shown by the hydrothermal products formed in successive processes: pyrite formation → silicic alteration → potassic alteration (K-feldspar formation) → carbonatation → phyllic (sericitic) alteration. All these indicate acidic to neutral fluids during the early hydrothermal phases when temperature was around 175 °C and when the most intense pyrite deposition and silicic alteration occurred. Upon cooling the fluids gradually turned to a neutral-alkaline character, when potassic alteration (i.e. formation of K-feldspar/adularia), carbonatation and phyllic alteration prevailed. According to experimental data, smectite, illite-smectite, illite and K-feldspar (all present in the Certej ore deposit) form at neutral-alkaline pH values, while halloysite, kaolinite (both only sporadically present at Certej) and pyrophyllite precipitate from acidic fluids (Meunier, 2005).

Change from acidic to neutral and slightly alkaline conditions upon cooling is also favorable for the transport of high gold concentrations in a magmatic fluid of low salinity and high sulphur activity (Gammons & Williams-Jones, 1997; Heinrich, 2005). The K concentration in the fluid should have increased during early hydrothermal processes (when acidic-neutral solutions affected the K-bearing rock-forming minerals and K was released from them) to allow the formation of K-feldspar and sericite by K-metasomatism (when the solutions turned to alkaline-neutral). As K was consumed during potassic and phyllic alteration processes, the formation of late NH_4-bearing illite (*i.e.* tobelite, identified in the Certej samples, Gál et al., 2010) could occur (Higashi, 2000).

Ore mineral characteristics also suggest chemical changes during evolution of hydrothermal processes. Zoning and overgrowth structures associated with variable As content of pyrite grains, for example, can be assigned to compositional changes of the parent hydrothermal solutions during crystal growth (e.g. As depletion due to the crystallization or As-bearing sulphides). The presence of xenomorphic grains of pyrite suggest post-crystallization re-dissolution phenomena affecting initial idiomorphic crystals, as the porous-textured grains also indicate. Moreover, reaction coronas were observed at some of the xenomorphic grain boundaries endorsing the same conclusion.

Sphalerite veins from the lower levels of the Certej deposit show variable colours suggesting variation of minor element (Fe) and trace element (Mn, Cd) contents and possibly a slow growth process similar to that described by Di Benedetto et al. (2005).

T-P constraints of the hydrothermal fluids

Most information on thermal conditions of hydrothermal process was obtained from microthermometric data. The latter indicate a temperatures range for the hydrothermal solutions at Certej between 179 and 317 °C (Table 14.1).

As Fe content in sphalerite is pressure-dependent, *e.g.* decreases with increasing pressure (Lusk et al., 1993), Fe-content zoning of investigated particular sphalerite crystals at Certej (Fig.14.7) suggests pressure oscillations in the hydrothermal system, at least during the growth of those particular crystals.

Pressure conditions, at which the hydrothermal fluid evolved, can be constrained theoretically from calculated fluid inclusion salinities (acc. to Steele-MacInnis et al., 2012), i.e. 0.18-5.41 mass% $NaCl_{eq}$. The corresponding pressure range would be 6.8-135.3 bar. This large range of values suggest that pressure conditions were extremely variable (probably both in time and space) during hydrothermal alteration and mineralization. Shifts between open system conditions (characterized by hydrostatic pressure) to closed-system conditions (when lithostatic pressure prevailed), due to alternating hydrothermal brecciation/fracturing (pressure release) and fracture healing (pressure build-up) could be an explanation for the wide range of calculated pressures.

Spatial variation of characteristics of the hydrothermal processes

The higher frequency of primary fluid inclusions in quartz grown at depth than in that formed at shallower levels suggests that hydrothermal fluid availability was also higher (Roedder, 1962) in the lower levels of the Certej ore deposit, consistent with ascendant fluid flux paths.

Comparing the main mineral associations from Certej and Dealul Grozii with the Corbett & Leach (1998) chart, some temperature and pH constraints can be drawn. Higher temperature and neutral pH at depth, and medium to lower temperature and neutral to alkaline PH at shallow level respectively, were characteristic for Certej ore deposit (*sensu strictu*). The mineral associations at present-day surface reveal slightly more alkaline and slightly hotter hydrothermal fluids. At similar temperatures, hydrothermal fluids in the Dealul Grozii part of the ore deposit (eastern part of the area) seem to have been more alkaline than in the western part of the area (*i.e.* Coranda).

Origin of the hydrothermal fluids

According to O and H stable isotope data ($\delta^{18}O$= ~7 ‰ to ~40 ‰ $_{SMOW}$ and $\delta^{34}S$ =0 ‰ $_{CDT}$), a dominantly juvenile origin of the mineralizing hydrothermal solutions was assumed for the Certej ore deposit (Alderton et al., 1998; Alderton & Fallick, 2000).

The data obtained for inclusions in quartz and sphalerite plot in the salinity *vs.* homogenization temperature discriminating diagram (Lattanzi, 1991; Hedenquist el al., 1998 and Naden et al., 2005) in a field assigned partly to epithermal fluids of magmatic (juvenile) origin and partly to a domain with meteoric affinity (Fig. 18.1). Such behaviour is interpreted by Heinrich (2005) as representing a mixing domain

between meteoric and juvenile waters. Most likely at Certej the juvenile epithermal fluids have been continuously admixed with meteoric waters.

Further indications on the origin of hydrothermal fluids are provided by the ore mineral assemblages. The association of telluride minerals with native tellurium indicates direct magmatic input to the mineralizing solutions (Fadda et al., 2005). The formation of Te-phases in earlier phases of the mineralizing process at Certej marks a more substantial juvenile input. Later, the addition of meteoric water changed the whole hydrothermal system.

Ore formation. Synthetising the results, Te minerals (except for melonite) precipitated earliest, followed by sulphides and finally sulphosalts. More than one generation of pyrite and sphalerite has been formed. Generally, adularia predates ore mineral formation. As gold was not found in the studied samples, its position in the genetical sequence cannot be discussed. The identified Au-bearing minerals (petzite, nagyágite and sylvanite) precipitated in the early stage.

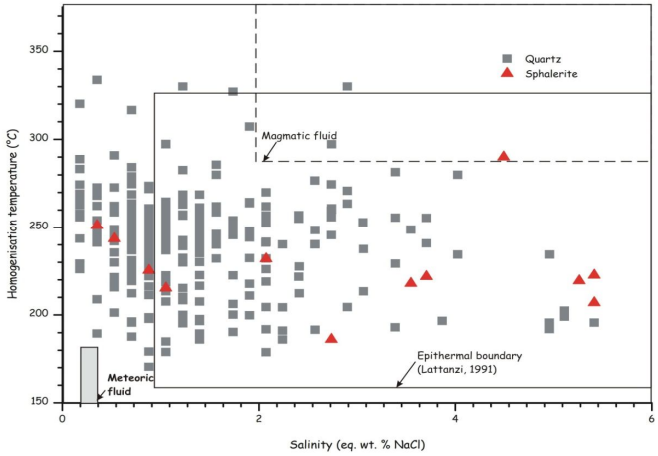

Fig. 18.1. Distribution of quartz- and sphalerite-hosted fluid inclusion homogenization temperatures in function of calculated salinity values at Certej as compared with metoric water and juvenile water domains (acc. to Lattanzi, 1991; Hedenquist el al., 1998;Naden et al., 2005).

Sulphur and tellurium fugacity. Constraints on sulphur fugacity and tellurium fugacity values can be inferred from the Afifi et al. (1998) diagram (Fig. 18.2). The relevant mineral phases present in the Certej ore deposit that support fugacity interpretation are pyrite, native gold, Ni-telluride (melonite), Hg-telluride (coloradoite) and Ag-telluride (hessite). According to their stability field, log fS_2 ranges from –6.8 to –11.5 and log fTe_2 from 7.5 to 14.5. These values are characteristic for the sulphidation status. Evolution of Te *vs.* S fugacity in the Certej hydrothermal system is shown by the timing of Te-bearing minerals and sulphides/sulphosalts, respectively. The Te fugacity value decreases in time, while S fugacity increases.

Boiling. There are numerous evidences of boiling in the mineralizing hydrothermal system at Certej. Formation of hydrothermal breccias in epithermal environments is usually accepted as proof of boiling. An increase in fluid pressure may result in hydraulic fracturing and, thus, in a sudden drop in pressure leading to brecciation (Berger & Eimon, 1983; Cole & Drummond, 1986; Jobson et al., 1994; Jébrak, 1997).

Occurrence of adularia is another possible clue for boiling. The cause of adularia precipitation may be the release of CO_2 during boiling, thus causing increase of solution pH. Consequently, a shift from illite to K-feldspar stability field occurs (see e.g., Browne & Ellis, 1970; Browne, 1978; André-Mayer et al., 2002; Canet et al., 2011). However, the main evidence of boiling comes from the fluid inclusion data showing entrapment of heterogeneous fluids and variable fluid/gas ratios (Bodnar et al., 1985).

Organic matter. The presence of organic matter (organic carbon) in the Cretaceous host rocks provided most likely favorable local conditions for gold precipitation. Organic matter induces changes in the redox potential of hydrothermal solutions, shifting them from oxidative to reducing. Organic carbon may have additionally contributed to the precipitation of other ore and gangue minerals e.g., pyrite, chalcopyrite and barite, respectively.

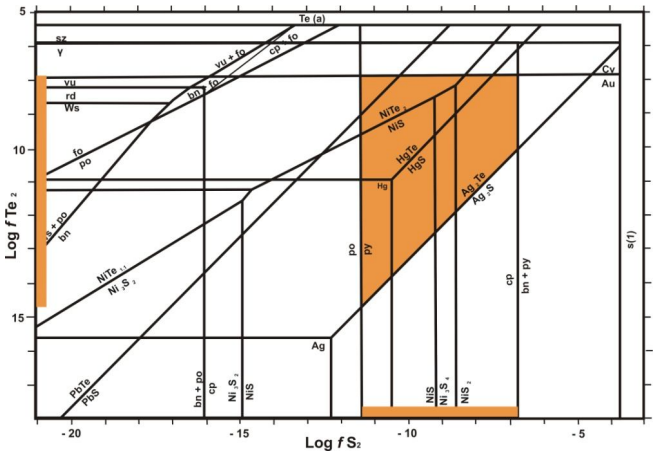

Fig. 18.2. Sulphur fugacity (fS_2) vs. tellurium fugacity (fTe_2) diagram of Afifi et al. (1988) showing the stability domains of various sulphide and telluride mineral phases.

Considerations regarding the genetic type of the Certej ore deposit

Low or intermediate sulphidation?

The Certej ore deposit was previously described as an epithermal deposit of 'low to intermediate sulphidation' type (Bundell et al., 2005; Kouzmanov et al., 2005). However, the results obtained during the present study require a slight revision of this earlier view.

The Certej ore deposit satisfies most of the criteria for intermediate sulphidation epithermal deposits (John, 1999, 2000; Hedenquist el al., 2000; John & Wallace, 2000; Einaudi et al., 2003; Sillitoe & Hedenquist, 2003 and Gemmell, 2004) i.e. abundant sericite, ore mineral assemblage containing sphalerite, galena, tetrahedrite and tellurides, low Fe content in sphalerite (0.05-0.125 mol% Fe – Raman spectroscopy data, and 0-0.67 mass% Fe – ED spectrometry data), hydrothermal quartz filling veins, breccias and geodes, and probably shallow (with respect the paleo watertable) mineralizing environment. In the sulphur fugacity *vs.* formation temperature diagram of Einaudi et al. (2003), the Certej ore deposit plots in the field of intermediate sulphidation (Fig. 18.3).

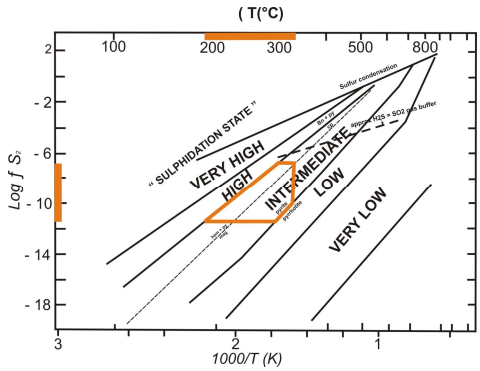

Fig. 18.3. Discrimination of different sulphidation states for epithermal ore deposits in the sulphur fugacity *vs.* temperature diagram of Einaudi et al. (2003). The position of the Certej ore deposit is marked with the orange polygon.

Carlin type?

The Carlin-type gold deposits have a complex origin involving both magmatic-hydrothermal ore forming processes and a sedimentary host rock (Muntean et al., 2011). Therefore, the features of Certej ore deposit support the question whether it might belong to this type. The main argument consists in the sedimentary nature of the rock hosting the mineralization (Cretaceous shales). These rocks provided a reducing environment for the metal-bearing hydrothermal fluids, ultimately determining gold precipitation. Some of the relevant features of the Certej Au deposit are compatible with a Carlin-type genesis because: a) the geodynamic setting of the Southern Apuseni Mountains is extensional at the time of mineralizing event (Miocene) and a previous subduction-related inherited overprint is envisaged (e.g. Roșu et al., 2004; Harris et al., 2013); b) the mineralization is mostly sediment-hosted; c) gold occurs as fine grains (*i.e.* "invisible" gold) associated with disseminated As-rich pyrite; d) fluid type (H_2O-NaCl dominant system with $CaCl_2$, $MgCl_2$ or KCl) and temperatures (179-317 °C) are at least partly compatible; e) a meteoric water component of the fluids is reasonably supposed; f) H_2S content in fluid inclusions (0-3.14 mol% at homogenization temperatures) is compatible with the Carlin-type Au deposits average.

However, at least two major characteristics of the Certej Au deposit do not fit with the classically described Carlin type (Hausen & Kerr, 1968): a) the sedimentary host rocks are not carbonatic, although sedimentary carbonatic components are present in the Cretaceous flysch sequence (*i.e.* carbonatic cement of some sandstones); b) the Certej ore deposit is obviously related to intrusive magmatic activity and the hydrothermal fluids are partly of juvenile origin.

In conclusion, although inconsistent with the classically described Carlin-type Au deposits, the Certej ore deposit can be classified as a Carlin-type deposit in a broader-sense. In this respect, an entirely non-juvenile origin of the mineralizing fluids and a carbonatic host-rock are not necessary conditions for ore genesis. This new classification intends to emphasize the sediment-hosted character of the Certej ore deposit, which is considered to define the ore genesis. Mixing between magmatic fluids and meteoric water has also been important to ore genesis at Certej. Penetration of meteoric water towards deeper levels via

breccia and faults lead to decrease of temperature and increase of pH. Such changes in the physical-chemical conditions may have contributed to precipitation of base metal sulphides.

Chapter 19. Conclusions

The Certej epithermal ore deposit related to Neogene magmatic activity in Southern Apuseni Mountains, in particular the intrusion of andesitic Băiaga body, shows specific features due to a complex interplay of geological, structural, mineralogical and physical-chemical factors.

The magma moving NW towards SE along a steeply dipping extensional shear plane provoked the intense fissuring and brecciation of the Cretaceous and Neogene sedimentary country rocks. This stress direction allowed later the penetration and circulation of mineralizing hydrothermal fluids. The K-Ar age of illite and adularia, minerals formed in the early stages, indicates the beginning of the hydrothermal processes ~12 Ma ago.

Besides the ore mineralization, the hydrothermal solutions have induced a predominantly K-metasomatism within the andesite body and, in particular, within the sedimentary host rocks nearby. It started with an earlier potassic alteration (formation of illite and K-feldspar) which graded, upon cooling, into a sericitic type (formation of fine-grained muscovite). However, locally, argillic process marks the waning stage of the hydrothermal process.

Most of the physical and chemical parameters of the fluids, such as the fluid/rock ratio, the amount and kind of volatile/semi-volatile elements, the pH and the temperature, largely varied during the hydrothermal activity. The composition and physical characteristics of the fluid inclusions show not only the general boiling conditions, at least in the earlier, hotter stages of the hydrothermal activity and at the deeper levels, but also the input of meteoric waters to the fluids of prevalently magmatic origin. This input could lead to significant variations in temperature and hydrothermal fluids concentration. Finally, aqueous fluids containing NaCl, KCl and CO_2 resulted. The Cretaceous shales, as main host rocks of the mineralization, additionally provided some amounts of nitrogen, methan and hydrogen sulphide.

The load of the hydrothermal fluids is reflected by the extremely wide range of minerals formed: sphalerite, pyrite, gersdorffite, melonite, stibnite, tetrahedrite, native Ag, hessite, sylvanite, coloradoite, altaite, tellurite, stützite, nagyágite, petzite, jarosite, aluminium-phosphate-sulphate minerals, anatase, quartz, calcite, dolomite, rhodochrosite, gypsum, barite. These minerals formed in a certain order. Te-minerals (except for melonite) precipitated earliest, followed by sulphides (pyrite, sphalerite and galena), then sulphosalts. Several generations of pyrite and sphalerite formed.

No native gold was found during this study however Au-bearing minerals petzite, nagyágite and sylvanite occur. Their precipitation seemed to have been favored by the reducing environment created in the Cretaceous shales, rich in organic matter.

The electron microprobe analysis, X-ray powder diffraction and in particular microthermometric and Raman spectroscopical investigations of fluid inclusions proved to be appropriate tools in reaching the aims of the study, i.e. “to unveil the specific genetic processes leading to the formation of the Certej intermediate sulphidation type, epithermal Au-rich ore deposit associated to the Neogene ’Băiaga’ andesite”.

The detailed field and analytical data at Certej ore deposit allowed a classification of the ore deposit, to infer the directions of hydrothermal fluid circulation, their physical and chemical evolution as well as the relation between the mineral content and the host-rocks. Among the multitude of minerals, several were described for the first time in the Certej ore deposit (native silver, native tellurium, gersdorffite, altaite, coloradoite, nagyágite, stützite, melonite, anatase, tellurite and APS minerals), and in the weathering zone of the mined ore (apjohnite, halotrichite, hexahydrite, copiapite, aluminocopiapite, pickeringite, jarosite, hydroniumjarosite, goethite, alunogen, gibbsite and voltaite). Melonite is recorded and described for the time in whole Romania.

The Certej ore deposit satisfies the criteria to be classified as ‘intermediate sulphidation epithermal ore deposits’ and not as ‘low-to-high sulphidation type’ as previously thought. Additional features support the inclusion of the Certej ore mineralization among the ‘Carlin-type’ ore deposits.

Acknowledgements

First of all I would like to thank Prof. Dr. Corina Ionescu for her careful and high-level professional guidance of this work and, not least, for her patiance, encouragements and help to overpass difficult moments inherently occurring during the elaboration of the final form of this thesis.

I acknowledge the precious help received from the DevaGold S.A. Company (European Goldfields) and the former Cuprumin Deva Company which facilitated access, fieldwork and sampling in the Certej underground and open pit mining areas.

I thank collectively the professional and administrative staff of the Department of Mineralogy, and the LRG research group within the Department of Petrology and Geochemistry of the Eötvös Lóránd University, Budapest for their permanent and friendly support during many years in carrying out a lot of laboratory and analytical work. Too, I highly benefited from the generous support of my colleagues from the Geology Department of the Babeş-Bolyai University, Cluj-Napoca. Not least, I was supported with kind and competent assistance by staff members of the Department of Mineralogy and Petrography, University of Miskolc, Hungary, where part of my analytical work was undertaken. Special thanks of mine go to the following persons who offered me more than expected technical and human support in a large variety of issues, including special analytical techniques and instruments, as well as data processing and analysis:

- Enikő Bali, Márta Berkesi, Boglárka Kis, Kalin Kouzmanov, Erzsébet Tóth and András Fall – advicing and consulting,
- Márta Berkesi and Tamás Váczi – Raman spectroscopy,
- Ferenc Lázár Forray – geochemical analyses, GPS and computer processing of data,
- István Gatter, Ferenc Molnár, Csaba Szabó and Ioan Pintea – fluid inclusion studies,
- Lucreţia Ghergari † – crystal morphology studies, investigation of clay minerals,
- Ferenc Kristály and Tamás Weiszburg – XRDP investigations,
- Ferenc Kristály and Norbert Zajzon – microprobe analysis,
- István Márton – field-work logistics, structural investigations, computer-assisted map construction,
- Zsuzsa Molnár – NAA investigations,
- Emilia Mosonyi – interpretation of structural data,
- Béláné Nagy – OES analyses,
- Zoltán Pécskay – K-Ar radiometric dating,
- Monica Mereu – computer-assisted map drawing.

Prof. Dr. Lucreţia Ghergari† helped me greatly in choosing and defining the topic and of the main research topics of this study. I am deeply endebted to her.

During the study years I benefited from the following mobility grants generously offered by the Hungarian Ministry of Education, the Koch Sándor Foundation, and the CEEPUS Program.

I also thank to all my friends who listend patiently my complaints over the years and who encouraged me in difficult moments.

Last but not least, I thank to my familiy without whose patience, understanding and love this work could not be accomplished.

Finally, I apologize to all persons who interacted with me in a positive and friendly manner during the study period and who are not nominally mentioned here just because innocent ignorance rather than because any bad feelings.

References

Ackner, J., 1855, Mineralogie Siebenbürgens. mit Geognostischen en Andeutungen Hermannstadt. Druck und Verlag von Theodore Steinhaussen, 392 p.

Afifi, A.M., Kelly, W.C., and Essene, E.J., 1988, Phase relations among tellurides, sulfides, and oxides. I. Thermochemical data and calculated equilibria; II. Applications to telluride-bearing ore deposits. Economic Geology, v. 83, p. 377-394 and 395-404.

Alderton, D.H.M., and Fallick, A.E., 2000, The Nature and Genesis of Gold-Silver-Tellurium Mineralization in the Metaliferi Mountains of Western Romania. Econ Geol, v. 95, p. 495-516.

Allan, M.M., and Yardley, B.W.D., 2007, Tracking meteoric infiltration into a magmatic-hydrothermal system. A cathodoluminescence, oxygen isotope and trace element study of quartz from Mt. Leyshon, Australia. Chem. Geol., v. 240, p. 343-360.

André-Mayer, A.-S., Leroy, J., Bailly, L., Chauvet, A., Marcoux, E., Grancea, L., Llosa, F., and Rosas, J., 2002, Boiling and vertical mineralization zoning. a case study from the Apacheta low-sulphidation epithermal gold-silver deposit, southern Peru. Miner. Deposita, v. 37, p. 452–464.

Apopei, A.I., Damian, G., and Buzgar, N., 2012, A preliminary Raman and FT-IR spectroscopic study of secondary hydrated sulfate minerals from the Hondol open pit (Metaliferi Mts., Romania). Rom. J. Min. Dep., v. 85, p. 1-6.

Apopei, A.I., Damian, G., Buzgar, N., Milovska, S., and Buzatu, A., 2014, New occurrences of hessite, petzite and stützite at Coranda-Hondol open pit (Certej gold-silver deposit, Romania). Carpath. J. Earth Env. Sci, v. 9, p. 71-78.

Berbeleac, I., Popa, T., Ioan, M., Iliescu, D., and Costea, C., 1995, Main characteristics of Neogene volcanic-subvolcanic structures and hosted ore deposits in Metaliferi Mountains. Geol. Maced., v. 9, p. 51–60.

Berger, B.R., and Eimon, P., 1983, Conceptual models of epithermal precious metal deposits. In. W.C. Shanks (Editor), Cameron Volume on Unconventional mineral Deposits, AIME Soc. Mining Eng., p. 191-205.

Bodnar, R.J., Reynolds, T.J., and Kuehn, C.A., 1985, Fluid inclusion systematic in epithermal system. Rev. Econ Geol, v. 2 - Geology and geochemistry of epithermal systems, p. 73-88.

Bodnar, R.J., and Vityk, M.O., 1994, Interpretation of microthermometric data for H_2O-NaCl fluid inclusions. In: Fluid inclusions in minerals, methods and applications, B. De Vivo and M. L. Frezzotti (Eds.), Virginia Tech. Blacksburg, VA, p. 117-130.

Browne, P.R.L., 1978, Hydrothermal alteration in active geothermal fields. Annu. Rev. Earth Pl. Sc., v. 6, p. 229–250.

Browne, P.R.L., and Ellis, A.J., 1970, The Ohaki-Brodlands hydrothermal area, New Zealand. Mineralogy and related geochemistry. Am. J. Sci., v. 269, p. 97-131.

Bundell, D., Arndt, N., Cobbold, P.R., and Heinrich, C., 2005, Geodynamics and ore deposit evolution in Europe. Ore Geol. Rev., p. 360.

Canet, C., Franco, S.I., Prol-Ledesma, R.M., González-Partida, E., and Villanueva-Estrada, R.E., 2011, A model of boiling for fluid inclusion studies. Application to the Bolaños Ag–Au–Pb–Zn epithermal deposit, Western Mexico. J. Geochem. Explor., v. 110, p. 118-125.

Ciobanu, C.L., Cook, N.J., Tămaş, C.G., Leary, S., Manske, S., O'Connor, G.V., and Minuţ, A., 2004, Tellurides-gold-base metal associations at Roşia Montană. The role of hessite as gold carrier. In: Cook, N.J. and Ciobanu, C.L. (Eds.), IGCP International Field Workshop Project 486, Alba Iulia, 2004, Intern. As. Geol. Ore Dep. Guidebook Series, v. 12, p. 187-202.

Cioflică, G., Jude, R., and Lupulescu, M., 1992, Cupriferous metallization processes associated with Upper Cretaceous–Eocene magmatites from Romania. Rom. J. Mineral., v. 76, p. 1–16.

Cioflică, G., Jude, R., Lupulescu, M., and Ducea, M., 1996, Lower crustal origin of the Late Cretaceous–Eocene arc magmatism in the western part of the South Carpathians, Romania. In: Terranes of Serbia, Knežević, V., Krstić, B. (Eds.), Faculty of Mining and Geology and Committee for Geodynamics of Serbian Academy of Science and Art, Belgrade, p. 103-107.

Cole, D.R., and Drummond, S.E., 1986, The effect of transport and boiling on Ag/Au ratios in hydrothermal solutions. a preliminary assessment and possible implications for the formation of epithermal precious-metal ore deposits. J. Geochem. Explor., v. 25, p. 45-79.

Cook, N.J., Ciobanu, C.L., Capraru, N., Damian, G., and Cristea, P., 2005, Mineral assemblages from the vein salband at Săcărâmb, Golden Quadrilateral, Romania. II. Tellurides. Miner. Petrol., v. 43, p. 47-55.

Corbett, G.J., and Leach, T.M., 1998, Southwest Pacific gold-copper systems. Structure, alteration and mineralization. Soc. Econ. Geo. Spec. Pub., v. 6, p. 238.

Deer, W.A., Howie, R.A., and Zussman, J., 2003, Rock-Forming Minerals, 3A. 2nd ed. Geol. Soc. London, 712 p.

Di Benedetto, F., Bernadini, G.P., Costagliola, P., Plant, D., and Vaughan, D.J., 2005, Compositional zoning in sphalerite crystals. Am. Mineral., v. 90, p. 1384 – 1392.

Einaudi, M.T., Hedenquist, J.W., and Inan, E.E., 2003, Sulphidation State of Fluids in Active and Extinct Hydrothermal Systems. Transition from Porphyry to Epithermal Environments. Econ. Geol., Sp.Publ., 10, p. 285-313.

Fadda, S., Fiori, M., and Grillo, S.M., 2005, Chemical variations in tetrahedrite-tennantite minerals from the Furtei epithermal Au deposit, Sardinia, Italy: Mineral zoning and ore fluids evolution. Bulgarian Academy of Sciences, Geochemistry, Mineralogy and Petrology, IGCP Project 486, 2005 Field Workshop, Kiten, 14-19 September 2005, v. 43, p. 79-84.

Fichtel, J.E., 1780, Beytrag zür Mineralgeschichte von Siebenbürgen, I-II. Nürnberg, 158 p.

Gál, Á., Kristály, F., Szakács, A., Molnár, F., and Weiszburg, T.G., 2010, Illite and kaolinite in the Coranda low sulphidation type epithermal deposit, Apuseni Mts., Romania. Acta Mineral.-Petrogr., Abstr. series, v. 6, p. 295.

Gammons, C.H., and Williams-Jones, A.E., 1997, Chemical mobility of gold in the porphyry–epithermal environment. Econ. Geol., v. 92, p. 45–59.

Gemmell, J.B., 2004, Low and intermediate sulphidation epithermal deposits. 24ct Gold Workshop, CODES Sp. Publ., v. 5, p. 57-63.

Ghiţulescu, T.P., and Socolescu, M., 1941, Etude géologique et minière des Monts Métallifères (Quadrilatère aurifère et régions environmnantes). An. Inst. Geol. Rom., v. 21, p. 181-464.
Gifkins, C.C., Allen, R.L., and McPhie, J., 2005, Apparent welding textures in altered pumice-rich rocks. J. Volcanol. Geotherm. Res., v. 142, p. 29-47.
Giggenbach, W.F., 1984, Mass transfer in hidrothermal alteration systems – A conceptual approach. Geochim. Cosmochim. Acta, v. 48, p. 2693-2711.
—, 1997, The origin and evolution of fluids in magmatic-hydrothermal systems. In Barnes, H. L., ed., Geochemistry of hydrothermal ore deposits, 3rd ed., John Wiley & Sons New York, p. 737−796.
Goldstein, R.H., and Reynolds, T.J., 1994, Systematics of fluid inclusions in diagenetic minerals: SEPM (Soc. Sedim. Geol.), Short Course Notes, v. 31, p. 1-213.
Götze, J., 1998, Geochemistry and provenance of the Altendorf feldspathic sandstone in the Middle Bunter of the Thuringian basin (Germany): Chem. Geol., v. 150, p. 43-61.
Götze, J., Plötze, M., Graupner, T., Hallbauer, D.K., and Bray, C.J., 2004, Trace element incorporation into quartz: A combined study by ICP-MS, electron spin resonance, cathodoluminescence, capillary ion analysis, and gas chromatography. Geochim. Cosmochim. Acta, v. 68, p. 3741-3759.
Götze, J., Plötze, M., and Habermann, D., 2001, Cathodoluminescence (CL) of quartz: origin, spectral characteristics and practical applications. Mineral. Petrol., v. 71, p. 225-250.
Gubareva, D.B., Stenina, N.G., and Gutakovsky, A.K., 1999, Crystal chemical features of water and impurity incorporation in natural quartz. Mater. Struct., v. 6, p. 124-128.
Harangi, S., and Lenkey, L., 2007, Genesis of the Neogene to Quaternary volcanism in the Carpathian–Pannonian region. role of subduction, extension and mantle plume: GSA Spec. Pap., v. 418, p. 67–92.
Harris, C.T., Peacey, J.G., and Pickles, C.A., 2013, Selective sulphidation and flotation of nickel from a nickeliferous laterite ore. Minerals Eng., v. 54, p. 21-31.
Hashimoto, T., 2008, An overview of red-thermoluminescence (RTL) studies on heated quartz RTL application to dosimeter and dating. Geochronometria, v. 30, p. 9-16.
Hausen, D.M., and Kerr, P.F., 1968, Fine gold occurrence at Carlin, Nevada. : in Ridge, J.D., ed., Ore deposits of the United States, 1933–1967: New York, Am. Inst. Mining Eng., v. 1, p. 908–940.
Hedenquist, J.W., Arribas, A., Jr., and Reynolds, T.J., 1998, Evolution of an intrusion-centered hydrothermal system: Far Southeast-Lepanto porphyry and epithermal Cu-Au deposits, Philippines. Econ. Geol., v. 93, p. 373−404.
Hedenquist, J.W., Arribas, R.A., and Gonzalez-Urien, E., 2000, Exploration for epithermal gold deposits. Rev. Econ. Geol., v. 13, p. 245-277.
Heinrich, C.A., 2005, The physical and chemical evolution of low-salinity magmatic fluid at the porphyry to epithermal transition. A thermodynamic study: Miner. Deposita, v. 39, p. 864−889.
Herbich, F., 1873, On the systematics of eruptive rocks in Transylvania (in Hungarian). Erdélyi Múzeum Egyesület Évkönyve, v. 6, p. 141-146.
Higashi, S., 2000, Ammonium-bearing mica and mica / smectite of several pottery stone and pyrophyllite deposits in Japan: their mineralogical properties and utilization. Appl. Clay Sci., v. 16, p. 171-184.
Hosaka, M., Miyata, T., and Sunagawa, I., 1995, Growth and morphology of quartz crystals synthesized above the transition temperature. J. Cryst. Growth, v. 152, p. 300-306.
Inkey, B., 1885, Geological and mining conditions of Săcărâmb. Magyar Természettud. Társ., v. VIII, p. 175. (in Hungarian).
Ioan, M., Şimon, G., and Alderton, D.H.M., 1993, A new occurrence of tellurides at Măgura Hondol, Metaliferi Mountains, Romania. Rom. J. Mineral., v. 76, p. 25.
Ionescu, C., and Hoeck, V., 2010, Mesozoic ophiolites and granitoids in the Apuseni Mts. RO2 Field trip guide, IMA-2010. Acta Mineral. Petrogr. (Szeged). Field Guide Series, v. 20, p. 1-45.
Jébrak, M., 1997, Hydrothermal breccias in vein-type ore deposits. A review of mechanisms, morphology and size distribution. Ore Geol. Rev., v. 12, p. 111-134.
Jobson, D.H., Boulter, C.A., and Foster, R.P., 1994, Structural controls and genesis of epithermal gold-bearing breccias at the Lebong Tandai mine, Western Sumatra, Indonesia. J. Geochem. Explor., v. 50, p. 409-428.
John, D.A., 1999, Magmatic influence on characteristics of Miocene low-sulphidation Au-Ag deposits in the northern Great Basin. Geol. Soc. Am. Abstr. Program, v. 31, p. A-405.
—, 2000, Magmas and Miocene low-sulphidation Au-Ag deposits in the northern Great Basin. Geol. Soc. Am. Abstr. Program, v. 31, p. A-250.
John, D.A., and Wallace, A.R., 2000, Epithermal gold-silver deposits related to the northern Nevada rift, *in* Cluer, J.K., Price, J.G., Struhsacker, E.M., Hardyman, R.F., and Morris, C.L., ed., Geol.ore deposit+ 2000. The Great Basin and beyond. Symp. Proceed., Geol. Soc. of Nevada, Reno,v. 1, p. 155-175.
Kawasaki, M., 1995, Effect of Al upon the morphology of synthetic quartz crystals. J. Cryst. Growth, v. 155 p. 75-80.
—, 2003, Growth-induced inhomogeneities in synthetic quartz crystals revealed by the cathodoluminescence method. J. Cryst. Growth, v. 247, p. 185-191.
Koch, A., 1885, Critical overview of minerals from Transylvania (in Hungarian). Orvos-Természettud. Társ., Cluj, p. 211.
Kouzmanov, K., Ivăşcanu, P., and O'Connor, G., 2005, 1-1: Porphyry Cu–Au and epithermal Au–Ag deposits in the southern Apuseni Mountains, Romania: South Apuseni Mountains district: Lat. 46°03′ N, Long. 22°58′ E. Ore Geol. Rev., v. 27, p. 46–47.
Lattanzi, P., 1991, Applications of Fluid Inclusions in the Study and Exploration of Mineral Deposits. Eur. J. Mineral., v. 3, p. 689-701.

Leary, S., O'Connor, G.V., Minuţ, A., Tămaş, C.G., Manske, S., and Howie, K., 2004, The Roşia Montană ore deposit: in Cook, N.J., and Ciobanu, C.L., eds., Au-Ag-telluride deposits of the Golden Quadrilaterial, Apuseni Mts., Romania: IGCP International Field Workshop Project 486, Alba Iulia, 2004, International Association for the Geology of Ore Deposits, Guidebook Series 12, p. 89-98.

Lusk, J., Scott, S.D., and Ford, C.E., 1993, Phase relations in the Fe–Zn–S system to 5 Kbars and temperatures between 325 and 150 °C: Econ. Geol., v. 88, p. 1880–1903.

Meunier, A., 2005, Hydrothermal process-thermal metamorphism. Springer New York, 415 p.

Milu, V., Leroy, J.L., and Piantone, P., 2003, The Bolcana Cu–Au ore deposit (Metaliferi Mountains, Romania): first data on the alteration and related mineralisation. Compt. Rend. Geosci., v. 335, p. 671-680.

Monecke, T., Kempe, U., and Götze, J., 2002, Genetic significance of the trace element content in metamorphic and hydrothermal quartz: a reconnaissance study. Earth Planet. Sci.Lett., v. 202, p. 709-724.

Muntean, J.L., Cline, J.S., Simon, A.C., and Longo, A.A., 2011, Magmatic-hydrothermal origin of Nevada's Carlin-type gold deposits. Nat. Geosci., v. 4, p. 122-127.

Naden, J., Kilias, S.P., Leng, M.J., Cheliotis, I., and Shepherd, T.J., 2005, Do fluid inclusions preserve δ18O values of hydrothermal fluids in epithermal systems over geological time? Evidence from paleo- and modern geothermal systems, Milos island, Aegean Sea. Chem. Geol., v. 197, p. 143–159.

Pécskay, Z., Lexa, J., Szakács, A., Balogh, K., Seghedi, I., Konečný, V., Kovács, M., Márton, E., Kaličiak, M., Széky-Fux, V., Póka, T., Gyarmati, P., Edelstein, O., Roşu, E., and Zeč, B., 1995, Space and time distribution of Neogene-Quaternary in the Carpatho-Pannonian Region. Acta Vulcanol., v. 7, p. 15-28.

Pécskay, Z., Lexa, J., Szakács, A., Seghedi, I., Balogh, K., Konečný, V., Kovács, M., Márton, E., Zelenka, T., Póka, T., Fülöp, A., Panaiotu, C., and Cvetković, V., 2006, Geochronology of Neogene-Quaternary magmatism in the Carpathian arc and Intra-Carpathian area: a review. Geol. Carpath., v. 57, p. 511-530.

Pricopie, M., Tuşa, L., Cristea, P., Căpraru, N., and Márton, I., 2004, Geology of the Certej project and a new model foy high-grade gold mineralisation hosted within the Dealu Grozii-Hondol parameter (Certej deposit). IAGOD: Guidebook Series, v. 12, p. 105-110.

Primics, G., 1888, Geological observations in the territory of the Cetraş Mountains. Földtani közlöny, v. XVIII, p. 5-31. (in Hungarian).

Robb, L., 2005, Introduction to ore-forming processes, Wiley-Blackwell, Oxford, 373 p.

Roedder, E., 1962, Studies of fluid inclusions I: Low Temperature application of dual purpose freezing and heating Stage. Econ. Geol., v. 57, p. 1045-1061.

Roşu, E., Pécskay, Z., Ştefan, A., Popescu, G., Panaiotu, C., and Panaiotu, C.E., 1997, The evolution of the Neogene volcanism in the Apuseni Mountains (Romania): Constrain from new K-Ar data. Geol. Carpath., v. 48, p. 353-359.

Roşu, E., Seghedi, I., Downes, H., Alderton, D.H.M., Szakács, A., Pécskay, Z., Panatoiu, C., Panatoi, C.E., and Nedelcu, L., 2004, Extension-related Miocene calc-alkaline magmatism in the Apuseni Mountains, Romania: Origin of magmas. Schweiz. Miner. Petrog., v. 84, p. 153-172.

Rudnick, R., and Gao, S., 2003, Composition of the continental crust. In: Holland, H. and Turekian, K. (Eds.), Treatise on Geochemistry, v. 3, p. 1-64.

Saccani, E., Nicolae, I., and Tassinari, R., 2001, Tectono-magmatic setting of the ophiolites from the South Apuseni Mountains (Romania). Petrological and geochemical evidence. Ofioliti, v. 26, p. 9–22.

Seghedi, I., Downes, H., Szakács, A., Mason, P.R.D., Thirlwall, M.F., Roşu, E., Pécskay, Z., Márton, E., and Panaiotu, C., 2004, Neogene–Quaternary magmatism and geodynamics in the Carpathian–Pannonian region: a synthesis. Lithos, v. 72, p. 117-146.

Sillitoe, R.H., and Hedenquist, J.W., 2003, Linkages between volcanotectonic settings, ore-fluid compositions, and epithermal precious-metal deposits. Soc. Econ. Geol. Sp.Publ., v. 10, p. 315-343.

Şimon, G., Alderton, D.H.M., and Bleser, T., 1994, Arsenian nagyágite from Săcărâmb, Romania; a possible new mineral species. Mineral. Mag., v. 58, p. 473-478.

Şimon, G., Alderton, D.H.M., Stumpfl, E.F., and Bleser, T., 1995, Tellurantimony in Romania; first occurrences in Europe. Mineral. Petrol., v. 53, p. 115-124.

Steele-MacInnis, M., Lecumberri-Sanchez, P., and Bodnar, R.J., 2012, HokieFlincs_H_2O-NaCl: A Microsoft Excel spreadsheet for interpreting microthermometric data from fluid inclusions based on the PVTX properties of H_2O–NaCl. Comput. Geosci., v. 49, p. 334-337.

Sunagawa, I., Berhardt, H.-J., and Schmetzer, K., 1999, Texture formation and element partitioning in trapiche ruby. J. Cryst. Growth, v. 206, p. 322-330.

Swamy, V., Saxena, S.K., Sundman, B., and Zhang, J., 1994, A thermodynamic assessment of silica phase diagram. J. Geophys. Res., v. 99B, p. 11787–11794.

Udubaşa, G., 1993, TX constraints of ore parageneses with some case studies. Rom. J. Min., v. 76 p. 7-13.

Udubaşa, G., Istrate, G., and Vălureanu, M., 1979, Metallogenesis in the Coranda-Hondol area, Metaliferi Mountains. D.S. Inst. Geol. Geofiz., v. 67 (2), p. 197-232.

Udubaşa, G., Strusievicz, R.O., Dafin, E., and Verdeş, G., 1992, Mineral occurrences in the Metaliferi Mts., Romania. Rom. J. Min., v. 75 p. 1-35.

Van den Kerkhof, A.M., and Hein, U.F., 2001, Fluid inclusion petrography. Lithos, v. 55, p. 27-47.

von Hingenau, O.F., 1857, Geologisch-bergmännische Skizze des Bergamtes Nagyág und seiner nächsten Umgegend. Jahrb. der k.k. Geol. Reichs., v. 8, p. 82-143.